properties are a consequence of strong hybridization of the $5f$ orbitals on the uranium atom with neighboring anion p orbitals and possibly also with nearest-neighbor uranium d orbitals to form the bonding states. A consideration of the geometry of the NaCl structure and the f, p, and d orbitals shows that the energy gained from the in-plane 2D bonding arrangement in the oblate configuration (relative to [001]) is greater than that gained from bonding arrangements normal to the plane in the prolate configuration, because of the smaller number of bonding orbitals in the latter case. If this "bonding" energy is greater than the crystal-field energy, this would explain why the ground state of the uranium atom is different from that expected from crystal-field considerations, as revealed by the form factor measurements,[2] and also the Ising-like nature. The bonding picture also explains why the correlations between the spins on the uranium ions within the (001) sheets are strong, since this interaction is transmitted via the direct overlap of neighboring orbitals, whereas the interaction between the sheets must rely on the weaker indirect conduction-electron–exchange mechanism. We thus have a system in which the magnetic ordering is not dominated completely either by indirect exchange between localized moments (as in the $4f$ series) or by an interaction primarily between *spins* of itinerant electrons (as in the $3d$ metals), but in which the bonding involving $5f$ electrons coupled with the strong spin-orbit interaction plays an important role in the development of long-range magnetic order. Further experimental and theoretical investigations of these intriguing systems are in progress.

We are grateful to R. L. Hitterman for experimental assistance. This work was supported by the U. S. Department of Energy.

[1]A. T. Aldred and D. J. Lam, in *The Actinides: Electronic Structure and Related Properties*, edited by A. J. Freeman and J. B. Darby (Academic, New York, 1974), Vol. I, Chap. 3.

[2]G. H. Lander, M. H. Mueller, D. M. Sparlin, and O. Vogt, Phys. Rev. B 14, 5035 (1976).

[3]G. H. Lander, D. M. Sparlin, and O. Vogt, in *Magnetism and Magnetic Materials—1976*, AIP Conference Proceedings No. 34, edited by J. J. Becker and G. H. Lander (American Institute of Physics, New York, 1976). Similar anomalies have been found in measurements on UN; see W. J. L. Buyers, T. M. Holden, E. C. Svensson, and G. H. Lander, in Proceedings of the International Conference on Neutron Inelastic Scattering, Vienna, October 1977 (International Atomic Energy Agency, to be published).

[4]M. P. Schulhof, P. Heller, R. Nathans, and A. Linz, Phys. Rev. B 1, 2304 (1970).

[5]R. J. Birgeneau, J. Skalyo, and G. Shirane, Phys. Rev. B 3, 1736 (1971), and J. Appl. Phys. 41, 1303 (1970).

Spatial Condensation of Strain-Confined Excitons and Excitonic Molecules into an Electron-Hole Liquid in Silicon

P. L. Gourley and J. P. Wolfe
University of Illinois at Urbana-Champaign, Urbana, Illinois 61801
(Received 14 November 1977)

By direct spatial imaging and spectral analysis of recombination luminescence we have observed in silicon (1) the drift of photoproduced excitons from the crystal surface into a strain potential well; (2) ideal-gas behavior of the strain-confined excitons in the well between 25 and 5 K; (3) a real-space condensation near $T = 4$ K which defines the first-order gas-liquid phase transition; and (4) luminescence from excitonic molecules.

In this Letter we report observations of luminescence from free excitons (FE), excitonic molecules (EM), and electron-hole liquid (EHL) confined within a strain-induced potential well inside a pure Si crystal. Above $T = 5$ K the FE luminescence exhibits a Gaussian spatial profile $\exp(-\alpha x^2/kT)$ expected for an ideal gas in a parabolic potential well, $V = \alpha r^2$. Near 4 K the spatial profile abruptly narrows and luminescence from the liquid phase appears, indicative of a first-order phase transition. By this means we have produced for the first time in Si a large volume of EHL with greatly enhanced lifetime. We report the first images of these excitonic phases in Si.

An appealing aspect of the strain-confinement technique is that it produces a well-defined spatial distribution of excitons in the semiconductor.

In this way the unknown spatial inhomogeneities associated with surface excitation are avoided.[1] Above the critical temperature of the liquid the volume of the excitonic gas in the strain well is independent of excitation power so that the gas density may be directly controlled by the excitation level. Consequently high densities of excitons have been produced without resorting to pulsed excitation.

Figure 1 is a photograph of the FE recombination luminescence emanating from an ultrapure Si crystal ($N_A - N_D < 10^{12}$ cm^{-3}) at 15 K, showing the drift of excitons from the crystal surface, where they are created, to a potential minimum near the top of the sample. Only FE luminescence is observed at this temperature. The crystal is stressed from above along the ⟨100⟩ direction by a carefully rounded ($R \approx 5$ cm) steel plunger. The strain distribution is similar to that previously reported[2] for Ge, although the sheer-stress maximum $\sigma_{max} \simeq 50$ kg/mm^2 at 0.3 mm inside the surface is much larger in this case.[3]

The image was produced by an infrared-sensitive vidicon as previously described.[4,2] The sample is excited on the back 4 mm × 4 mm face by an argon laser beam ($\lambda = 5145$ Å), which is completely absorbed within 10 μm of the surface and is not detected on the images. The right photograph shows a side view through a 45-deg mirror adjacent to the sample. As indicated by the relative intensities, most of the photoproduced excitons are eventually confined within the strain potential well.

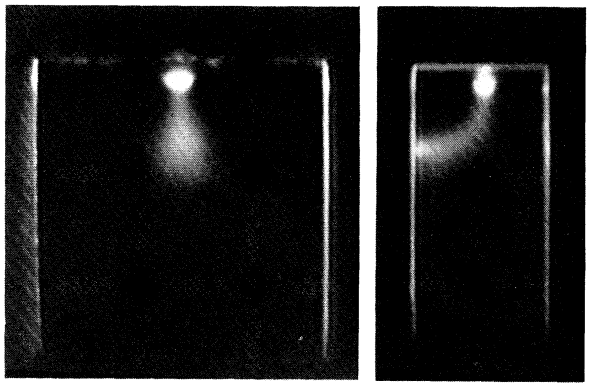

FIG. 1. Face and side views of the exciton luminescence from a 4 mm × 4 mm × 1.8 mm Si crystal at $T \simeq 15$ K, showing explicitly the migration of excitons from the excited surface to the potential well. The absorbed cw laser power is $P_{ab} \simeq 50$ mW. Crystal boundaries are defined by scattered luminsecence. The left photo is a view through the 4 mm × 4 mm (010) face with the laser defocused. The right photo is a side view with the focused laser beam incident on the left surface.

The spatial extent and profile of the strain-confined excitonic gas can be understood by treating the excitons as an ideal gas in a parabolic potential well. From the equipartition theorem, $\langle V \rangle = \alpha \langle r^2 \rangle = \frac{3}{2} kT$, and thus the radial extent of the gas is proportional to $T^{1/2}$. The spatial profile of the gas is quantitatively measured by slowly scanning a sharply focused image of the crystal across a narrow slit masking the Ge photodetector. The shape of the profile is in agreement with the predicted form $I(x) = I_0 \exp(-\alpha x^2/kT)$. In Fig. 2, we plot the full width at half-maximum (FWHM) of the shape as a function of temperature. Between 22 and 5 K the observed temperature dependence agrees reasonably well with the predicted $T^{1/2}$ form.

Near 4 K the luminescence profile abruptly contracts, indicating the first-order gas-liquid phase transition. This interpretation is confirmed by the simultaneous onset of the characteristic electron-hole–liquid recombination luminescence, as shown in Fig. 2(b) and Fig. 3.

Figure 3 displays the luminescence spectra

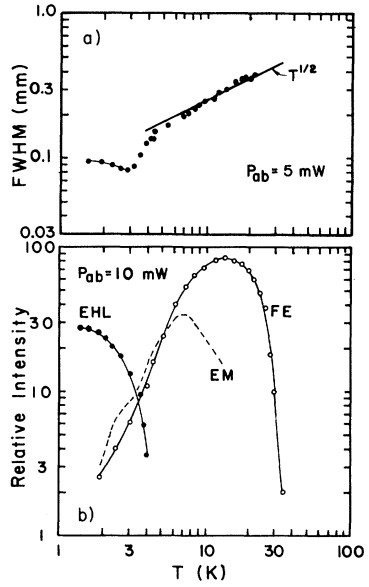

FIG. 2. (a) Spatial extent of the luminescence from the potential well vs T. Above $T = 5$ K, an ideal gas behavior is observed. Below $T = 4$ K, the FE gas has condensed into an EHL. The monochromator was removed to permit purely spatial (no spectral) imaging with a resolution of 0.04 mm. (b) Relative intensities of the three phases obtained with 1-meV spectral resolution.

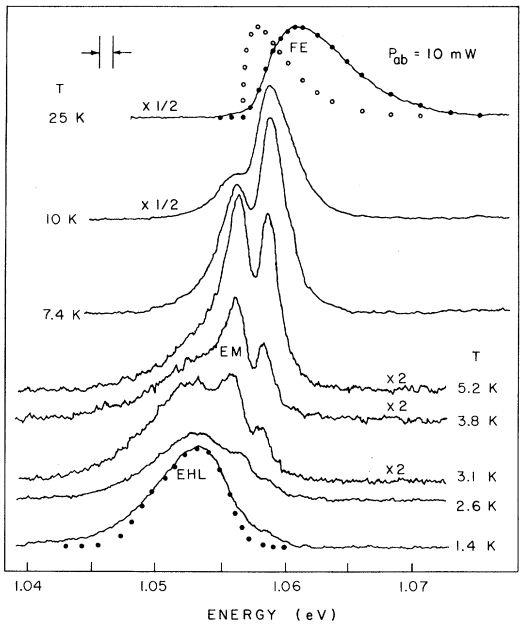

FIG. 3. Temperature dependence of the luminescence from the potantial well, showing the evolution of the three phases: EHL, EM, and FE. The maximum stress is about 55 kg/mm^2.

emanating from the potential well as a function of temperature. (Emission from the drifting excitons, Fig. 1, has been masked.) There are three distinct peaks in these spectra, which we interpret as emission from FE, EM, and EHL. At the highest temperature (25 K) only the FE peak is observed. At the lowest temperature (1.4 K) emission from the EHL is dominant. The relative intensities of FE and EHL have been plotted versus temperature in Fig. 2(b). Similar measurements at higher excitation levels (10–100 mW) indicate a threshold temperature $T \simeq 4$ K for formation of the strain-confined liquid. This value is much less than the critical temperature 14.3 K calculated by Vashishta, Das, and Singwi[5] for the FE-EHL transition in the high-stress limit. An interesting possibility here is that the association of excitons into molecules acts to depress the critical temperature of the liquid-gas (FE-EM) transition.

The extra peak between the FE and EHL energies which occurs at intermediate temperatures is likely due to EM, as recently observed under pulsed excitation in uniformly stressed Si by Kulakovsky and Timofeev.[6] We have found that at 4.2 K and for excitation power less than 10 mW the intensity of the new luminscence line increases quadratically with the FE intensity, as expected for biexcitons. A characteristic feature of biexciton luminescence is the long low-energy tail, corresponding to a distribution of final FE kinetic energies. We have carried out a preliminary line-shape analysis of the EM line similar to the method of Cho,[7] and find a biexciton binding energy $\simeq 1$ meV. Figure 3 shows that at the highest temperature the biexcitons are completely dissociated into free excitons.

To our knowledge this is the first time that all three phases have been observed under steady-state excitation. Previous studies[8,9] of the liquid-gas phase diagram in unstressed Si did not reveal the presence of biexcitons. Undoubtedly spatial confinement and reduced EHL binding energy, both effected by the potential well, favor production of EM. Exciton and molecular binding energies will also be modified by the strain due to reduced hole mass.

The line shape of the FE luminescence is explained by an extension of the ideal-gas ideas previously mentioned. Instead of using the usual free-particle density of states $D(E) \sim E^{1/2}$ we consider the exciton in the three-dimensional potential well $V(r) = \alpha r^2$. The energy levels are $E = \hbar\omega(n + \frac{3}{2})$ with degeneracy $\frac{1}{2}(n+1)(n+2)$. It follows that the density of states is $D(E) = E^2/2(\hbar\omega)^3$. In Fig. 3 the fit of the FE luminescence at 25 K by $E^2 \exp(-E/kT)$ is excellent (solid points). For comparison, the usual $E^{1/2}\exp(-E/kT)$ function applicable to excitons in the unstressed case is plotted (open circles). From Fig. 2(a) we find $\alpha = 4$ eV/cm^2 and $\hbar\omega = 10^{-7}$ eV.

The density of the EHL can be extracted from the luminescence line shape, provided the degeneracies $d_{e,h}$ of the conduction and valence bands are known. Under ⟨100⟩ stress the degeneracy of the conduction-band minimum is reduced from six to two, and the degeneracy of the valence-band maximum is reduced from two to one. It is known[10] that for an applied uniaxial stress greater than 15 kg/mm^2 the EHL will occupy only the lowest two conduction bands. The EHL occupies only one hole band above about 40 kg/mm^2.

As shown below, the stress maximum in the potential well is $\simeq 50$ kg/mm^2, where $d_e = 2$ and $d_h = 1$. Therefore the density n of the EHL is obtained by fitting the EHL luminescence spectrum by the shape

$$I(h\nu) = A \iint dE\, dE' D_e(E) D_h(E') f_e(E) f_h(E') \times \delta(h\nu - E - E' - E_0),$$

where $h\nu$ is the photon energy, $D_{e,h}$ are the con-

duction- and valence-band densities of states, E_0 is the minimum photon recombination energy of the liquid, and $f_{e,h}$ are the Fermi functions with Fermi energies $E_F^{e,h} = (\hbar^2/2m_{e,h})(3\pi^2 n/d_{e,h})^{3/2}$. We use the density-of-states masses $m_e = 0.322m_0$ and $m_h = 0.235m_0$, corresponding to the high-stress limit. As in the zero-stress case this simple theoretical line shape (solid circles, bottom trace of Fig. 3) does not fit the data perfectly. The fit corresponds to $n_\gamma = 3.7\times10^{17}$ cm^{-3} which is in reasonable agreement with the calculated[5] high-stress, zero-temperature value 4.7×10^{17} cm^{-3} and is considerably lower than the measured unstressed value $n_\alpha = 3.3\times10^{18}$ cm^{-3}. The low EHL density under stress is a result of the reduced band degeneracies.

Figure 4 identifies the EHL luminescence emanating from various regions of the crystal at low temperature, $T = 1.4$ K. The diffuse luminescence labeled α is from droplets of EHL created near the crystal surface by the defocused laser beam. The bright spot beneath the contact stress is a large volume of strain-confined liquid, labeled γ. The γ-EHL luminescence peak shifts in energy directly with stress and displays a narrower linewidth indicating the reduced liquid density. The α-EHL spectrum is similar to that reported previously[11] for unstressed Si; however, the α-FE line is shifted to lower energy (-6 meV) due to the small strain near the crystal surface. Using previous uniform-stress data,[10] we determine $\sigma_{max} \simeq 50$ kg/mm^2 from the observed γ-EHL energy shift.

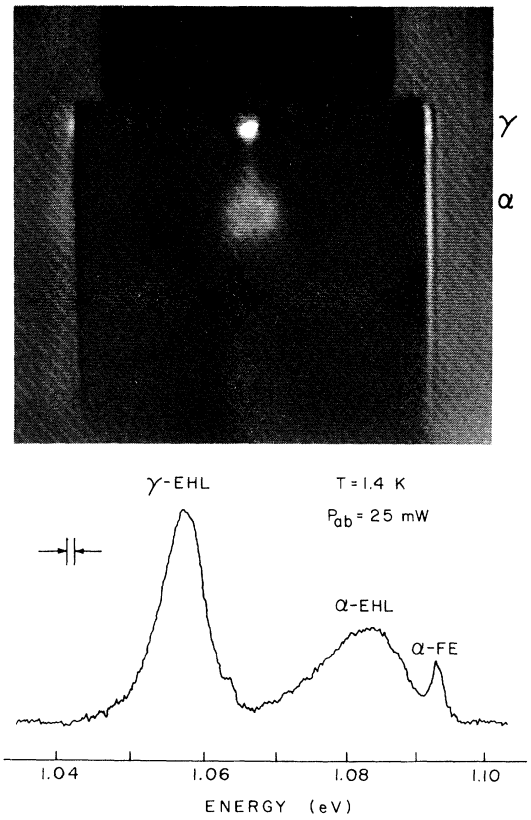

FIG. 4. (a) Luminescence from EHL in the stressed Si crystal at 1.4 K. The sample is backlit with a tungsten lamp to better display the crystal and stress-rod boundaries. The stress is slightly less than for Fig. 3. (b) Spectrum through a vertical slit centered on the potential well.

Finally, we have measured the lifetime of the strain-confined EHL following a short intense excitation pulse from a GaAs laser (100 ns at 10 W). The γ-EHL decay time is 2.0 μs compared to our measured α-EHL decay $\lesssim 0.19$ μs. As in the case of Ge, the tenfold enhanced lifetime is a natural result of the lower EHL density.[12]

We conclude that the strain-confinement method is a practical means of controlling the excitonic phases in Si and can provide new information about the gas-liquid phase transition.

We thank E. E. Haller for providing us with the Ge detector crystal and the ultrapure Si sample. M. Greenstein provided necessary technical assistance. We acknowledge a valuable discussion with V. B. Timofeev and thank J. D. Dow for his comments.

This work was supported in part by the National Science Foundation under Grant No. DMR-76-01058.

[1]In Ge, experiments have shown that the volume of an EHL cloud expands with increasing focused-laser excitation; thus the excitation level is not a reliable control of the average pair density (FE + EHL).

[2]R. S. Markiewicz, J. P. Wolfe, and C. D. Jeffries, Phys. Rev. B 15, 1988 (1977); J. P. Wolfe, R. S. Markiewicz, S. M. Kelso, J. E. Furneaux, and C. D. Jeffries, to be published.

[3]A series of birefringence studies were performed on this sample to determine the optimum stress geometry. The metal plunger used here produces a large stress desirable for the Si crystal.

[4]J. P. Wolfe, W. L. Hansen, E. E. Haller, R. S. Markiewicz, C. Kittel, and C. D. Jeffries, Phys. Rev. Lett. 34, 1292 (1975).

[5]P. Vashista, S. G. Das, and K. S. Singwi, Phys. Rev. Lett. 33, 911 (1974).

[6]V. D. Kulakovsky and V. B. Timofeev, Pis'ma Zh. Eksp. Teor. Fiz. 25, 487 (1977) [JETP Lett. 25, 458

(1977)].

[7]K. Cho, Opt. Commun. 8, 412 (1973).

[8]A. F. Dite, V. D. Kulakovsky, and V. B. Timofeev, Zh. Eksp. Teor. Fiz. 72, 1156 (1977) [Sov. Phys. JETP (to be published)].

[9]J. Shah, M. Combescot, and A. H. Dayem, Phys. Rev. Lett. 38, 1497 (1977).

[10]B. M. Ashkinadze, I. P. Kretsu, A. A. Patrin, and I. D. Yaroshetskii, Fiz. Tekh. Poluprovodn. 4, 2206 (1970) [Sov. Phys. Semicond. 4, 1897 (1971)].

[11]See, for example, R. B. Hammond, T. C. McGill, and J. W. Mayer, Phys. Rev. B 13, 3566 (1976).

[12]J. P. Wolfe, R. S. Markiewicz, C. Kittel, and C. D. Jeffries, Phys. Rev. Lett. 34, 275 (1975).

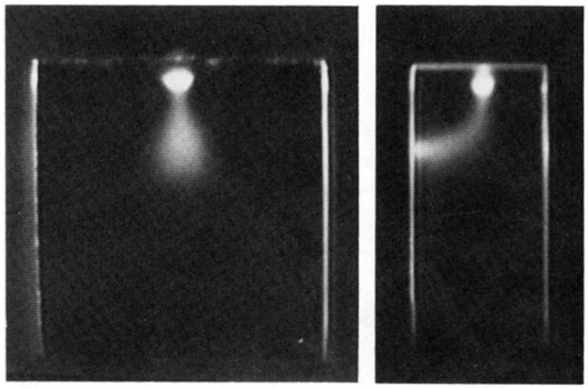

FIG. 1. Face and side views of the exciton luminescence from a 4 mm × 4 mm × 1.8 mm Si crystal at $T \simeq 15$ K, showing explicitly the migration of excitons from the excited surface to the potential well. The absorbed cw laser power is $P_{ab} \simeq 50$ mW. Crystal boundaries are defined by scattered luminsecence. The left photo is a view through the 4 mm × 4 mm (010) face with the laser defocused. The right photo is a side view with the focused laser beam incident on the left surface.

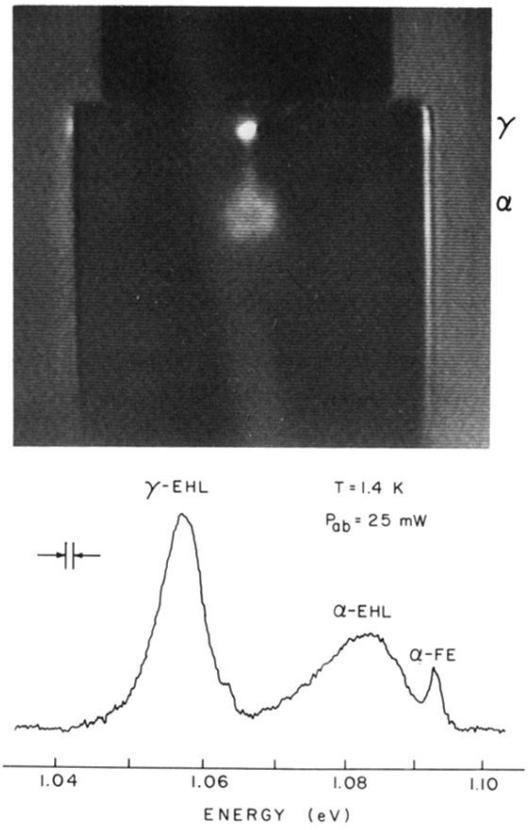

FIG. 4. (a) Luminescence from EHL in the stressed Si crystal at 1.4 K. The sample is backlit with a tungsten lamp to better display the crystal and stress-rod boundaries. The stress is slightly less than for Fig. 3. (b) Spectrum through a vertical slit centered on the potential well.